THE FAR-UV WAVELENGTH DEPENDENCE OF THE LUNAR PHASE CURVE AS SEEN BY LRO LAMP.

Y. Liu[1], K. D. Retherford[1], T. K. Greathouse[1], A. R. Hendrix[2], J. T. S. Cahill[3], K. E. Mandt[1], G. R. Gladstone[1], C. Grava[1], A. F. Egan[4], D. E. Kaufmann[4], W. R. Pryor[5]; [1]Southwest Research Institute, San Antonio, TX (yang.liu@swri.edu), [2]Planetary Sciences Institute, Tucson, AZ, [3]Johns Hopkins University Applied Physics Laboratory, Laurel, MD, [4]Southwest Research Institute, Boulder, CO, [5]Central Arizona University, Coolidge, AZ

Introduction: The Lunar Reconnaissance Orbiter (LRO) Lyman Alpha Mapping Project (LAMP) provides global coverage of both nightside and dayside of the Moon in the far ultraviolet (FUV) wavelengths between 57 and 196 nm [1]. The nightside observations use roughly uniform diffuse illumination sources from interplanetary medium Lyman-α sky glow and UV-bright stars so that traditional photometric corrections do not apply. In contrast, the dayside observations use sunlight as the illumination source where bidirectional reflectance is measured. The bidirectional reflectance is dependent on the incident, emission, and phase angles as well as the soil properties. Thus the comparisons of dayside mapping and nightside mapping techniques offer a method for cross-comparing the photometric correction factors because the observations are made under different lighting and viewing conditions. Specifically, the nightside data well constrain the single scattering albedo.

In this study, we discuss the FUV wavelength dependence of the lunar phase curves as seen by the LAMP instrument in dayside data. Our preliminary results indicate that the reflectance in the FUV wavelengths decreases with the increasing phase angles. This is similar to the phase curve in the UV-visible wavelengths as studied by Hapke et al. [2] and Sato et al. [3] using the LRO Wide Angle Camera (WAC) data, among other visible-wavelength lunar studies. Also, phase reddening at FUV wavelengths was observed; at UV-visible wavelengths, such phase reddening has been attributed to interparticle multiple scattering as the albedo increases [2, 3]. Finally, we report the derived Hapke parameters at FUV wavelengths for our study areas.

LAMP FUV Phase Curve: The LRO LAMP instrument is a push-broom style FUV imaging spectrograph with a spectral resolution of 2 nm and standard spatial resolution of ~ 250 m/pixel. Nominally pointed nadir, LAMP provides repeated observation of the Moon, enabling accumulation of FUV signal and higher data quality over the regions of interest. LAMP data were radiometrically calibrated to give the radiance factor $I/F(i, e, g)$, the radiance relative to a perfectly diffusing Lambert surface illuminated and viewed normally. Then the I/F were divided by the Lommel-Seeliger function, $LS = \cos i/(\cos i + \cos e)$, to get the reduced reflectance, where LS is a common factor in the radiative transfer equation for the theoretical photometric functions of particulate media.

To further improve signal/noise, we use 10 nm bandpasses combining five bins in the normal 2 nm products and lower spatial resolution (i.e., 4 km/pixel as compared to the standard 250 m/pixel) such that more photon events can be captured at each pixel for a given wavelength. The reduced reflectances at 165 nm against phase angles for sample mare and highlands regions are shown in Figure 1. For both sample mare and highlands, the reflectances decrease with increasing phase angles.

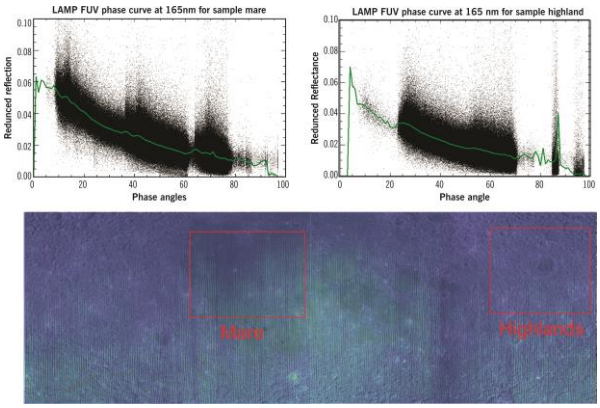

***Figure 1**. LAMP FUV phase curves at 165 nm for sample mare and highlands regions. The points correspond to individual pixels that have varying albedos at the same angles. The data were smoothed with a 0.5° wide moving spatial filter indicated by the green curves. The regions of interest are outlined by the red box in the LROC Wide Angle Camera (WAC) global mosaic of the Moon overlain by LAMP nightside Lyman alpha albedo maps with a transparency of 30%.*

Figure 2 shows the smoothed curves of reduced reflectances for 6 bandpasses together with the curves normalized at 15° for the sample mare and highlands regions, respectively. The phase curves have steeper slope at short wavelengths than the longer wavelengths, and this is so-called phase reddening [4]. We attribute this behavior to an effect similar to that produced by multiple scattering, but perhaps related to increased surface scattering, as in the FUV wavelengths, the reflectance lies in strong surface-scattering regime [5]. Also, our initial modeling tests indicate that the multiple scattering effects are negligible at small single scattering albedo values.

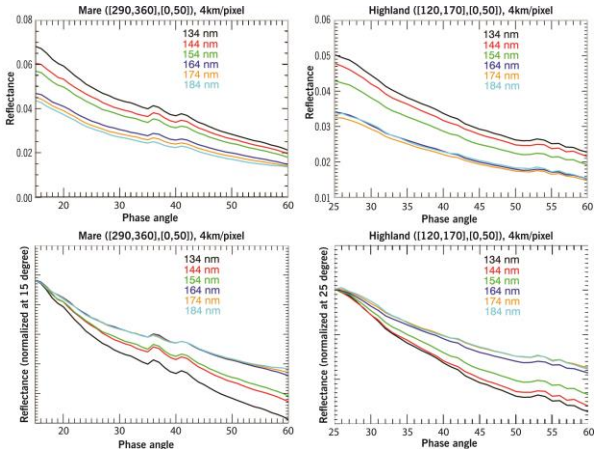

***Figure 2**. Phase reddening in the FUV wavelengths as observed by LRO LAMP. The top two panels show averaged reduced reflectances for all wavelengths (indicated by different colors) versus phase angle for sample mare (left) and highlands (right), and the bottow two panels show the same plots as above but normalized at 15° phase angle.*

Simplified Hapke Model: The full theoretical function for the bidirectional reflectance is [6]:

$$r = K\frac{w}{4\pi}\frac{\mu_0}{\mu_0+\mu}\{[1+B_{S0}B_S(g)]p(g)+H(\mu_0)H(\mu)-1\}\cdot[1+B_{C0}B_C(g)]\cdot S(i,\,e,\,g) \quad (1)$$

This equation can be simiplified under many circumstances. For example, Hapke et al. [2] made a series of simplifications on modeling LROC WAC data: (1) porosity, *K*, was set to be 1 as it cannot be uniquely determined by remote sensing, (2) the parameter, *c*, in the two-term Henyey-Greenstein phase function was set as 1 since there are no phase angles larger than 120° to detect forward scattering lobe of *p(g)*, (3) the roughness parameter, *S*, was set to be 1 as the range of phase angles is insufficient to determine roughness. For modeling the LAMP FUV data, we followed the similar assumptions, and additionally we set the shadow hiding and coherent backscattering to be 0 as the phase angles are larger than 15° in our data so that opposition effects can be ignored. Thus, the simplified Hapke bidirectional reflectance we used in this study is

$$r = \frac{w}{4\pi}\frac{\mu_0}{\mu_0+\mu}[p(g)+H(\mu_0)H(\mu)-1] \quad (2)$$

Dividing the bidirectional reflectance by π and the Lommel-Seeliger function to give the reduced reflectance

$$r\_Reduced = \frac{w}{4}[p(g)+H(\mu_0)H(\mu)-1] \quad (3)$$

where $r\_Reduced$ is equivalent to the LAMP reflectance values plotted in Figure 1.

Results and Future Work: Equation (3) was fitted to the phase curves for the sample mare and highlands for each wavelength. The example fitting results at wavelength 165 nm are shown in Figure 3, and the derived wavelength dependent single scattering albedo and asymmetric factor in the single-particle phase function for the sample mare and highlands are listed in Table 1. These parameters will be used to perform better photometric corrections for LAMP FUV reflectance data. Future work include deriving Hapke parameters of more refined mare and highlands areas and testing shadow hiding and coherent backscattering effects in FUV wavelengths when small phase angles are available in the areas investigated.

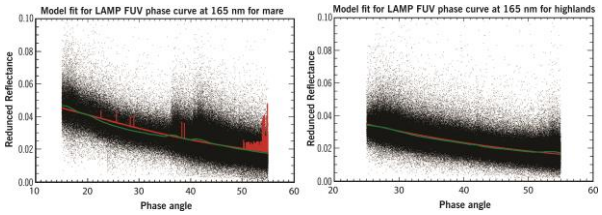

***Figure 3**. Hapke's model fit for phase curves at 165 nm for mare and highland regions of the Moon (a portion of phase angles were used for the fitting due to the data quality matter). Red lines is the model fit using Levenberg-Marquardt regression analysis algorithm. Green line is a running average 0.5 degree wide for comparison.*

Table 1. Retrieved wavelength dependent Hapke parameters for sample mare and highlands (*w* is the single scattering albedo, and *b* is the asymmetric factor for single-particle phase function)

Wavelength (nm)		134	144	154	164	174	184
Mare	*w*	0.092	0.085	0.079	0.065	0.061	0.058
	b	0.527	0.512	0.517	0.518	0.531	0.544
Highlands	*w*	0.087	0.083	0.075	0.060	0.058	0.060
	b	0.550	0.550	0.551	0.547	0.539	0.532

References: [1] Gladstone, G. R., et al., LAMP: The Lyman Alpha Mapping Project on NASA's Lunar Reconnaissance Orbiter Mission, Space Sci. Rev., 150, 161-181, 2010. [2] Hapke, B., B. Denevi, H. Sato, S. Braden, and M. Robinson (2012), The wavelength dependence of the lunar phase curve as seen by the Lunar Reconnaissance Orbiter wide-angle camera, J. Geophys. Res., 117, E00H15, doi:10.1029/2011JE003916. [3] Sato, H., M. S. Robinson, B. Hapke, B. W. Denevi, and A. K. Boyd (2014), Resolved Hapke parameter maps of the Moon, J. Geophys. Res. Planets, 119, 1775–1805, doi:10.1002/2013JE004580. [4] Gehrels, T., D. Coffeen, and D. Owings (1964), Wavelength dependence of polarization. III. The lunar surface, Astron. J., 69, 826–852, doi:10.1086/109359. [5] Wagner, J. K., et al., Atlas of Reflectance Spectra of Terrestrial, Lunar, and Meteoritic Powders and Frosts from 92 to 1800 nm, Icarus, 69, 14-28, 1987. [6] Hapke, B. (2012), Theory of Reflectance and Emittance Spectroscopy, 2nd ed., Cambridge Univ. Press, Cambridge, U. K.